Predicting ground reaction forces in running using micro-sensors and neural networks

D.C. Billing*†, C.R. Nagarajah*, J.P. Hayes*†, J. Baker‡

*Swinburne University of Technology, Hawthorn, Melbourne, Australia
†Cooperative Research Centre for microTechnology, Hawthorn, Melbourne, Australia
‡Australian Institute of Sport, Belconnen, Canberra, Australia

Abstract

Measurement of ground reaction force (GRF) in running provides a direct indication of the loads to which the body is subjected at each foot–ground contact, and can provide an objective explanation for performance outcomes. Traditionally, the collection of three orthogonal component GRF data in running requires an athlete to complete a series of return loops along a laboratory based runway, within which a force platform is embedded, in order to collect data from a discrete footfall. The major disadvantages associated with this GRF data collection methodology include the inability to assess multiple consecutive foot contacts and the fact that measurements are typically confined to the laboratory. The objective of this research was to investigate the potential for wearable instrumentation to be employed, in conjunction with artificial neural network (ANN) and multiple linear regression (MLR) models, for the estimation of GRF in middle distance running. A modular wearable data acquisition system was developed to acquire in-shoe force (ISF) data. Matched data sets from wearable instrumentation (source data) and force plate (target data) records were collected from elite middle-distance runners under controlled laboratory conditions for the purposes of ANN and MLR model development (MD) and model validation (MV).

In terms of statistical measures of prediction accuracy the MLR model was found to provide a superior level of accuracy for the prediction of the vertical and medio-lateral components of GRF and alternatively, the ANN model provided the most accurate predictions of the anterior–posterior component of GRF. The prediction accuracy of each component of GRF was found to be governed by the inherent signal variability, in which case the vertical and anterior–posterior components were more reliable and subsequently predicted significantly more accurately than the medio-lateral component.

The emerging capability for obtaining continuous GRF records from wearable instrumentation has the potential to permit unprecedented quantification of training stress and competition demands in running.

Keywords: artificial neural network, ground reaction force, multiple linear regression, running

Correspondence address:
Dan Billing
Defence Scientist in Health and Human Performance
Human Protection and Performance Division
Defence Science and Technology Organisation
506 Lorimer St, Fishermans Bend Vic 3207

Tel: +61 3 9626 8588
Fax: +61 3 9626 7830
E-mail: Daniel.Billing@dsto.defence.gov.au

Introduction

The mechanical means by which runners might achieve faster top running speeds include increasing stride frequency and/or increasing stride length. However, it has been demonstrated that faster top running speeds are not achieved by more rapid leg movements (stride frequency), but predominantly by increases in stride length conferred through the application of greater ground reaction force (GRF) (Weyand *et al*., 2000). From a purely mechanical perspective, GRF, along with other external forces acting on the body, including the subject's weight and wind resistance, ultimately dictate body motion and thus running performance (Putnam and Kozey, 1989). There are a number of limitations associated with the use of the traditional force platform GRF data collection methodology in running. Generally, the use of force plates necessitates laboratory data collection and the relatively small size of the platform itself (e.g. 0.9×0.6 m) often makes it difficult for the runner to contact its surface without altering the running stride (i.e. targeting), especially at high running speeds. In addition to the small size of the platform, many laboratory areas in which the platform is installed place unnatural constraints on the runner. The result is that most speeds tested are necessarily limited to those achieved by distance runners. A further limitation is that it is only possible to collect GRF data for a single support phase for each running trial.

A suitable alternative to the traditional force platform technique that could enable the continuous collection of three component GRF data in overground running is presently not available. This has placed significant limitations on the scientific evaluation of running and subsequently many questions relating biomechanics to performance remain unanswered. The recent advent of micro-sensors and miniature data acquisition systems has paved the way for the development and use of wearable, in-shoe pressure measurement systems. In-shoe pressure measurement circumvents many of the aforementioned limitations associated with the use of force platforms and has subsequently enabled the measurement of multiple successive foot steps and, importantly, allows for the collection of data outside a laboratory environment. Research has shown that summed pressure from a limited number of discrete in-shoe sensors (i.e. four to eight sensors), positioned under the major anatomical support structures of the foot, can provide a relatively close approximation of vertical GRF during running (Gross and Bunch, 1989; Hennig and Milani, 1995) and jumping (Walsh and Kanal, 1997). However, summed in-shoe pressure and vertical GRF measurements are not identical. Unlike force platform data, in-shoe measurements are subjectively moderated by a number of boundary conditions at the foot–shoe interface. The materials which surround the site from which measurements are made (i.e. shoe mid-sole) and the hot, humid and usually contoured in-shoe environment can result in subjective inter-trial and inter-subject sensor outputs. Also, with the role of the running shoe being to reduce, distribute and redirect the acting forces, its construction and material properties can have a significant influence on the loading pattern of different structures of the foot.

Many attempts have been made to develop sensors capable of determining the horizontal GRF components at the foot–shoe interface. In recent times the design, development and characterisation of an in-shoe tri-axial pressure measurement transducer have been reported (Razian and Pepper, 2003). Although this development represents a significant advance over transducers currently available for in-shoe measurements, further studies are required to validate the application of this sensor for use in measuring tri-axial pressures during running. The measurement of tri-axial pressure is not limited simply by sensor technology, as factors such as friction, non-planar force distribution, the deformable shoe reference frame, and space limitations for sensor deployment make direct measurement of such parameters challenging.

In light of these limitations a hybrid technique, utilising an artificial neural network (ANN) to establish a relationship between in-shoe pressure measurements and anterior–posterior GRF during walking, has been explored (Savelberg and de Lange, 1999). An ANN can be likened to a flexible mathematical function, which has many configurable internal parameters (Chau, 2001). To accurately represent complicated relationships among in-shoe pressure (source data) and the anterior–posterior component of GRF (target data), these internal parameters were

adjusted through a learning algorithm. To train the ANN, source data and corresponding target data were simultaneously presented to the network. A training algorithm was used iteratively to adjust the internal network parameters such that an optimal mapping was provided between source and target data. Provided that appropriate training data are used, the ANN can accept new sets of source data which it has not previously seen and predict the target data.

The objective of this research was to explore the application of this 'hybrid' technique in middle-distance running and expand predictions to all three components of GRF. Furthermore, this research also makes a direct comparison between an ANN model and a multiple linear regression (MLR) model (Draper and Smith, 1998), of which the MLR model is notably less complex and resource dependent. This research is focused towards middle-distance running owing to the inherent capacity for athletes participating in these events to sustain a relatively constant running velocity at a sub-maximal intensity. This is important as it enables the assessment of the wearable technique for the estimation of GRF at a running velocity equivalent to that experienced in competition, serving to maximise the face validity of this investigation.

Methods

Micro-sensor description and data logging instrumentation

Commercially available hydrocell sensors (paromed Vertriebs GmbH & Co. KG) were selected and utilised in this research. The overall sensor dimensions were 25.5 mm (length) × 20.5 mm (width) × 3 mm (thickness) with an active sensor area of 459 mm^2. Based on the principle that pressure in a fluid acts on all surfaces of an object in that fluid, the sensor design consisted of a piezoresistive micro-electro-mechanical system (MEMS) pressure sensor mounted within a constrained hydrocell (Chesnin *et al.*, 2000). The hydrocell consisted of an incompressible fluid (silicon oil) sealed in a polyurethane membrane (Leyerer *et al.*, 1997). The polyurethane membrane was further supported by a closed cell foam material surrounding the entire perimeter. The low density of the closed cell foam ensured that load was transferred to the polyurethane membrane. The sensor was then further reinforced on its two active surfaces by a layer of inelastic fabric which served to both protect the polyurethane membrane and reinforce the integrity of the entire packaged sensor. The hydrocell sensors were flexible and as such allowed adaptation to contours, such as that encountered at the foot–shoe interface, without impacting the quality of the readings.

The hydrocell sensors were designed to account for compressive and shear forces without discriminating between them. In this case forces may be applied simultaneously from both normal and tangential directions to either side of the polyurethane membrane of the hydrocell, resulting in an output from the MEMS piezoresistive pressure sensor which may be considered a resultant force. A number of authors (Tillman *et al.*, 2002; Perttunen *et al.*, 2000; Orlin and McPoil, 2000), who have utilised this sensor technology for in-shoe pressure measurement studies, have supported this statement.

A modular wearable data acquisition system consisting of a microcontroller module and a signal conditioning module was developed (Fig. 1). The microcontroller module, which was central to the system's functioning, consisted of a battery-operated microprocessor with an 8 bit analogue-to-digital converter, a 32 MB multimedia memory card for data storage, an LED function indicator, and a serial transceiver to facilitate communication with a host computer. The microprocessor (Hitachi H8/3664F) ran at a clock frequency of 9.83 MHz with a 3.3 V power supply. The microprocessor had 8 input channels of which 4 were used to sample the hydrocell pressure sensors. The microprocessor was initially programmed to sample each sensor at 1000 Hz and through the implementation of a firmware programmed two-point rolling average the resulting data acquisition rate was 500 Hz. Interfaced to the main electronics module was a separate signal conditioning module for the hydrocell sensors. This module, which was powered by the microcontroller module, in turn provided power to the hydrocell sensors and was responsible for the amplification of their output. A universal serial bus transceiver had also been developed: this directly interfaced to the microcontroller module and enabled downloading of data as well as uploading of firmware updates.

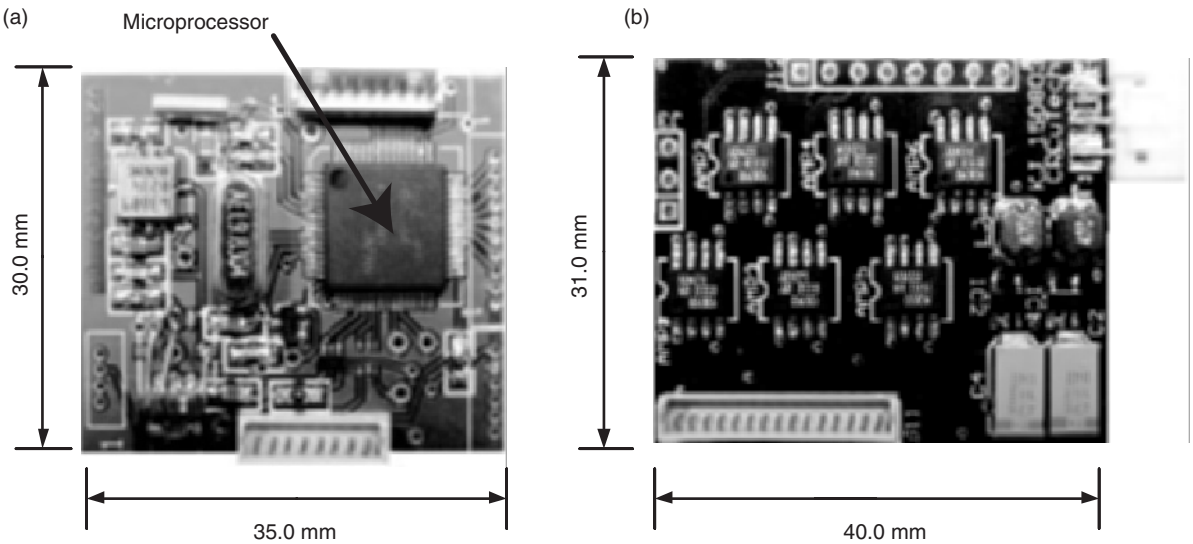

Figure 1 Data acquisition system including (a) microcontroller module and (b) signal conditioning module.

System calibration and deployment to subjects

In order to verify the operational characteristics and establish calibration factors for individual hydrocell sensors, a bench-top testing methodology was developed. Hydrocell sensors were individually calibrated under repeated dynamic compression loads using a Zwick Universal Tester (Zwick, Z010), as illustrated in Fig. 2. The purpose of this test was not to simulate loading characteristics at the foot–shoe interface, but to establish individual sensor calibration factors for the removal of inter-sensor variation. The calibration procedure involved the application of loads from 0–400 newtons (N) in steps of 50 N. A custom, solid aluminium force application tool (4 cm diameter) was developed which was contoured to reflect the shape characteristics of the human heel. The hydrocell sensor was compressed between the force application tool and a cylindrical metal plate measuring 15 cm in diameter. This resulted in the development of pressure within the polyurethane membrane of the hydrocell sensor, which was subsequently measured by the embedded MEMS piezoresistive pressure sensor.

In this study, four discrete hydrocell in-shoe force (ISF) sensors were deployed to the subject's left foot–shoe interface at the heel, first and third metatarsal head and hallux. These locations represent the major anatomical load bearing structures of the human foot in running (Hennig and Milani, 1995). Four sensors were implemented in this investigation in order to minimise the need for extensive support electronics and subsequently to ensure that the instrumentation remained unobtrusive to the subject. Discrete hydrocell sensors were embedded into a custom insole which was fabricated out of three layers of approved orthotic materials. Fig. 3 illustrates the layers of materials used for the insole fabrication and a completed insole detailing sensor locations. The hydrocell sensors were connected to a signal conditioning module and in turn to a data acquisition module via a flexible wiring harness. The data acquisition module and the signal conditioning circuitry module were incorporated into a semi-elastic belt, which was fastened around the subject's medial lumbar region.

Subjects, data collection procedure and pre-processing

Four elite (top ten national ranking) middle-distance (800 m and 1500 m) runners participated in this study after informed consent. Subject details are provided in Table 1. Data were collected from study participants within a range of running speeds (5–7 m s^{-1}) applicable to the athlete's average velocity in competition.

Data collection was conducted in the Biomechanics Laboratory at the Australian Institute of Sport. The Biomechanics Laboratory consisted of a 60 m runway of synthetic rubber (Rekortan) with two embedded Kistler force plates (Kistler Instrumente AG., Type 9287B) positioned midway and separated by an appropriate distance in order to obtain consecutive left and right footfalls. Force plates, each comprising a surface measuring area of 0.9 m × 0.6 m, were calibrated according to the manufacturer's instructions prior to use and set to operate at a data acquisition rate of 1000 Hz. Running velocity was measured instantaneously as the subject crossed between the force plates using a laser measurement system (LDM 300C, JENOPTIC-Group).

After an appropriate warm-up procedure, subjects were instructed to repeatedly run along the runway. They were not made aware of the location of the force plates to avoid targeting. Data from the wearable instrumentation were logged continuously whilst subjects completed a number of passes within a predetermined running velocity range (5–7 m s^{-1}) until a sufficient number of successful (direct contact with force plate and no visible alteration in running stride) trials were collected. During data collection subjects were made aware of their running speed for each trial. Before data collection began, subjects were instructed to complete a number of practice trials until the target running speed was consistently maintained. A video record was synchronised to the logging of the wearable instrumentation data for the purpose of confirming direct contact with the force platform and

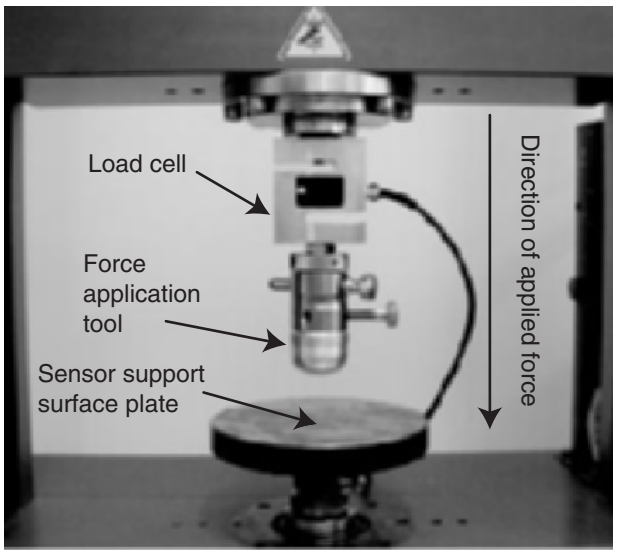

Figure 2 Force application tool and sensor support surface plate of the Zwick Universal Testing Machine.

Table 1 Subject details and average race speed recorded in the 2004 competition season.

Subject	A	B	C	D
Age (years)	27	20	20	18
Sex	M	F	M	M
Height (cm)	187	165	181	171
Body mass (kg)	72	49	58	56
Event speciality (m)	1500	1500	1500	800
Average race speed (m s^{-1})	6.69	5.86	6.77	7.26
5% below average race speed (m s^{-1})	6.35	5.57	6.43	6.89

Figure 3 (a) Layers used for the fabrication of the insole and (b) a completed insole detailing sensor locations.

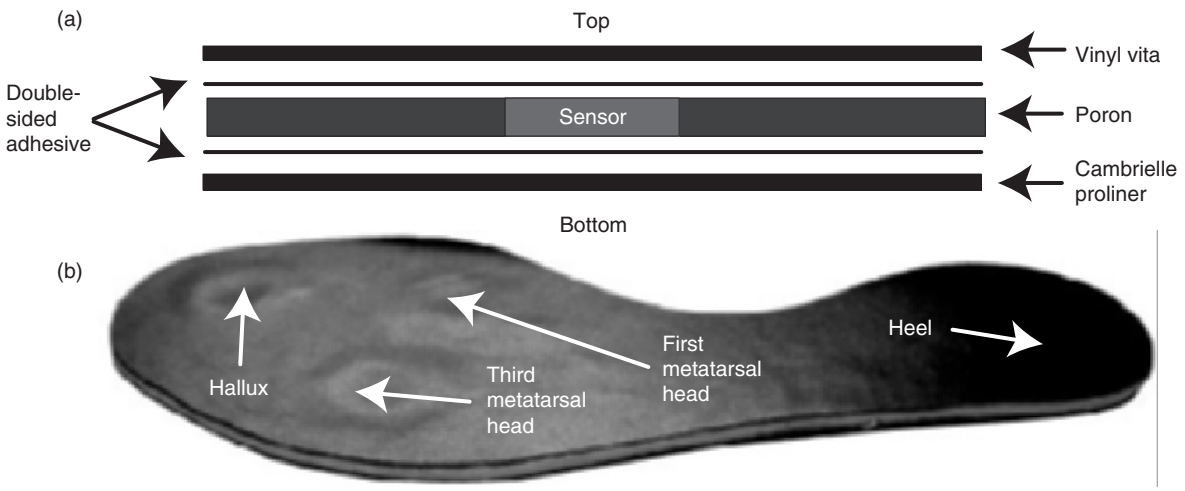

aligning matched wearable instrumentation data and force plate data during post-processing.

The minimum required number of successful left foot trials was nine for all four study participants (Table 2). The requirement for the collection of nine trials from each subject was implemented in order to enable the partitioning of the collective trial data for each subject into a model development (MD) and a model validation (MV) group (i.e. six trials for MD and three trials for MV). The overall trial data composition, obtained from the four study participants, enabled the prediction of all three components of GRF for all four study participants. An interpolation prediction scheme was applied for all results reported in this research. Interpolation is the condition under which the running speed of MV trials is within the running speed of those trials used for MD.

The final matched wearable and GRF data were then placed into matrices; calibration routines were performed on each data set. Baseline offsets were removed from the ISF data by calculating the median baseline value for the first 40 ms of each signal, prior to the onset of loading, and removing the magnitude of this value from the entire signal. Scale factors determined through bench-top calibrations for each individual ISF sensor were then applied to remove inter-sensor variation. Matching data sets from the wearable instrumentation and force plate records were then automatically aligned according to the first sample for each data set rising above a standardised threshold. This standardised threshold was determined through a number of steps. Firstly, the summed ISF signal was scaled by dividing its maximum value by the maximum vertical GRF value and subsequently multiplying all values by this scaling factor. Once scaled, a standardised threshold of 50 N was employed to align wearable instrumentation and force platform GRF records automatically.

Table 2 Subject running speed range and number of trials performed.

Subject	A	B	C	D	Overall
Mean speed (ms^{-1})	6.06	6.16	6.25	6.26	6.18
Minimal speed (ms^{-1})	5.35	5.86	5.83	5.99	5.76
Maximal speed (ms^{-1})	7.00	6.44	6.70	6.58	6.68
Number of left foot trials	9	9	9	9	36

Model implementation

MLR and ANN models were selected for investigation in this research. MLR was implemented to model the relationship between source data (ISF) and target data (GRF) by fitting a linear equation to observed data. An ANN was also configured to model the relationship between source and target data. However, owing to its flexible structure and many configurable internal parameters it had the added capability of capturing not only linear but also complex non-linear relationships. Calculations for both MLR and ANN models were carried out using the MATLAB® (The Mathworks, Natick, MA, USA) technical computing environment. Within the MATLAB® environment the 'Neural Network Toolbox' was employed for the implementation of the ANN.

Figs. 4 and 5 illustrate the MD and MV phases of the ANN and MLR model implementation respectively. The initial step of model execution involves the scaling of data collected for each running trial, which comprises matched and aligned source (ISF) and target (GRF) data for one independent support phase (foot–ground contact). This routine involves the independent scaling between zero and one of both source and target data for use as model inputs and outputs respectively. A selected group of trials were then partitioned into two subsets, where one trial group was used for the MD and another group was used for MV. In this research six trials have been employed for MD and three trials have been employed for MV. Previous research (Savelberg and de Lange, 1999) investigating the prediction of anterior–posterior GRF utilising an ANN found that as little as three to four MD trials are sufficient for the accurate prediction of a single MV trial. In this research three MV trials were employed in an effort to ascertain a more generalised indication of model performance.

Scaled ISF model inputs for a given trial were arranged in matrices and presented in a 'batched format' to corresponding GRF model outputs (target) for each time-series element of the signal. This process was repeated across the length of the time-series signal. In the case of MLR model, MD was completed by fitting a linear equation between the six trial MD source data set and the corresponding target data set, whereas ANN MD involved a learning process where in response to a given trial's source and

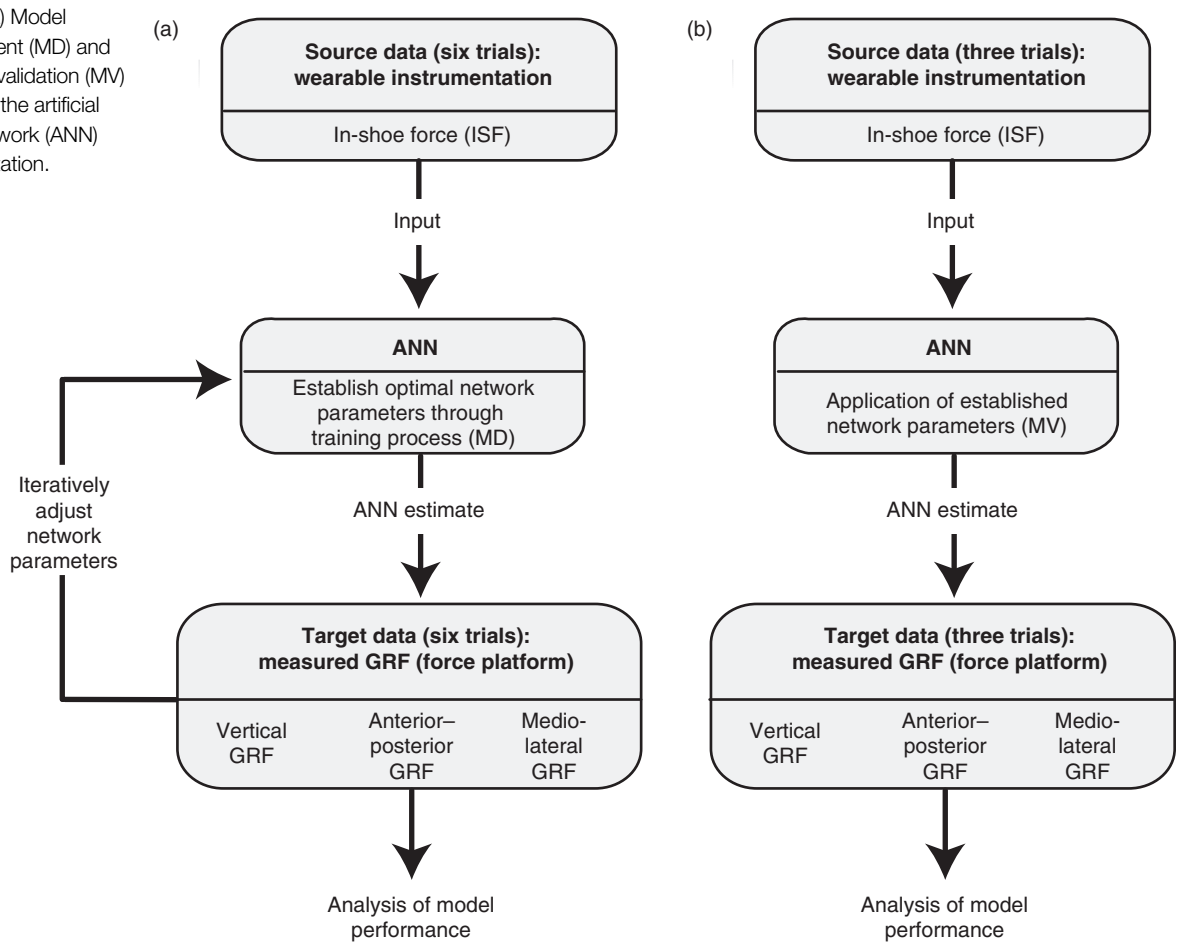

Figure 4 (a) Model development (MD) and (b) model validation (MV) phases of the artificial neural network (ANN) implementation.

target data set, the network learned to self-adjust its internal weights. These internal weights were adjusted after each complete MD trial was presented to the network, through an error back-propagation algorithm as illustrated in the ANN MD process in Fig. 4a. This process of updating the internal weights of the network is known as an epoch. The six MD trials were sequentially presented in an iterative manner, updating the internal weights of the network until the back-propagated error was minimised.

As opposed to mapping the relationship between source and target data sets, MV, a function evaluation process, involved the use of source data which were different from that used in MD and were designed to assess the predictive or generalisation capability of the ANN and MLR models against known targets (measured GRF). More specifically, utilising the MLR equation and the ANN internal weights established through the MD process, source data from the three MV trials were presented to and processed by the models, from which an estimation of the target data was provided. This estimation was then compared to the corresponding measured MV target data.

Importantly, from the first initiation (i.e. first epoch) to the completion of the ANN MD process, both MD and MV error (i.e. difference between estimated and measured target data) were assessed using the correlation coefficient (CC) and mean absolute error (MAE) measures. Each time the ANN MD process was initiated the internal weights of the network were randomly adjusted, resulting in unique MD and MV performance outcomes. In order to establish a generalised indication of ANN model performance the network was re-initialised and retrained 10 times with the average MD and MV error used as a guide to performance. Both MD and MV error were also evaluated

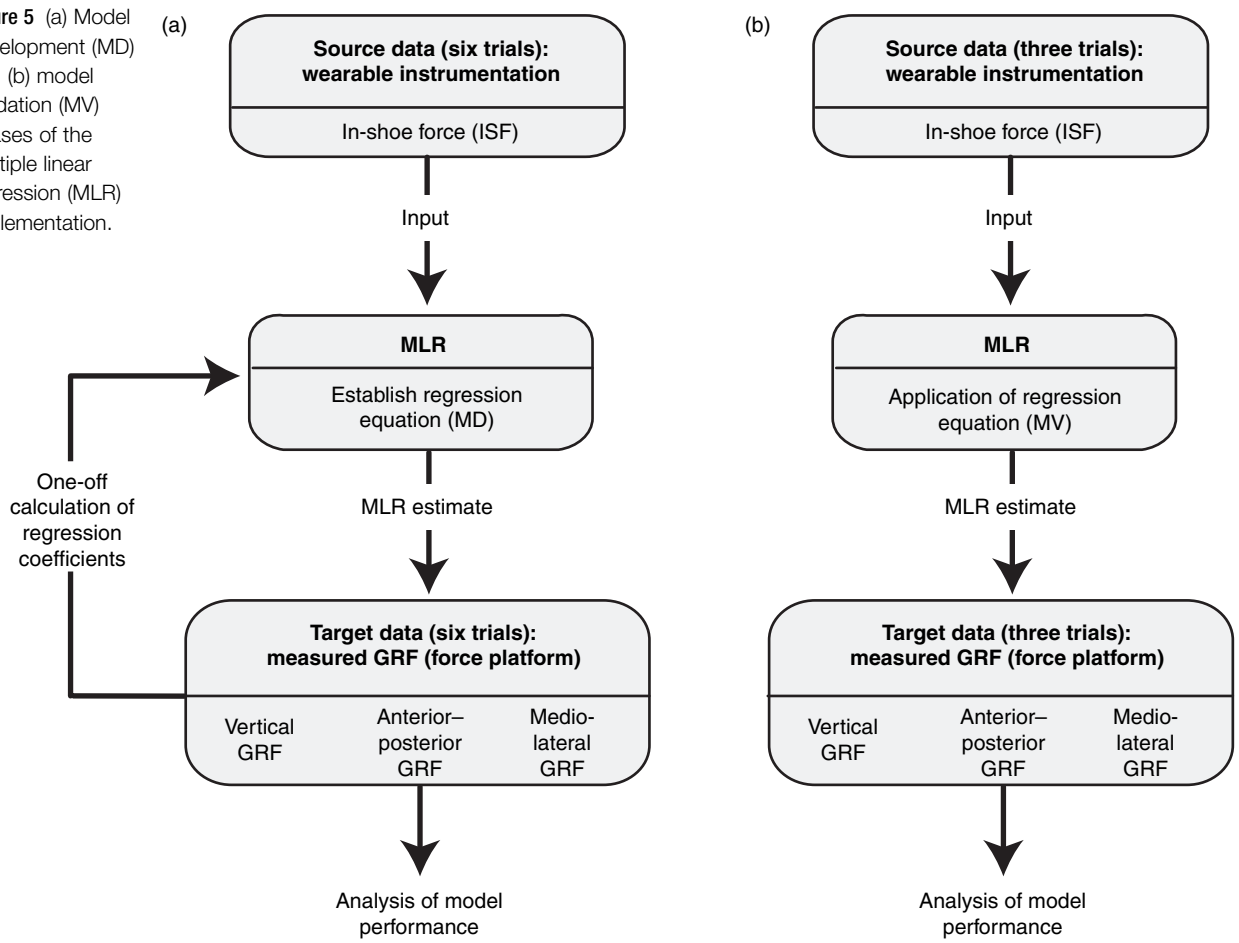

Figure 5 (a) Model development (MD) and (b) model validation (MV) phases of the multiple linear regression (MLR) implementation.

for the static MLR model. For the ANN and MLR models, CC and MAE measures were calculated across the entire MD (six trials) and MV (three trials) data sets. This provided for a more generalised indication of model performance. MD and MV error provided important insight into model performance, but MV error defined the ultimate utility. Therefore, the MV error was primarily used for the interpretation of model performance.

In this research a comprehensive optimisation procedure was undertaken for both the ANN and MLR models. In the case of the highly configurable ANN model, the network architecture was optimised by investigating various training algorithms, network structures, transfer functions and epoch paradigms. Furthermore, both the ANN and MLR models were optimised for the provision of historical data. Historical data points were incorporated as it was considered that at each instant in time the target data point of interest depended on both the corresponding source data point and source data points in the past. The characteristics of the optimised models are detailed in Table 3. To further analyse the relationship between measured and model estimates of GRF, a functional measure based on the average percentage error in the prediction of common GRF descriptor variables (summary parameters) across MD and MV data sets was also employed. Summary parameters measured for each component of GRF included: vertical GRF – contact time (s), impulse (N s) and vertical peak force (N); anterior–posterior GRF – braking time (s), propulsive time (s), braking impulse (N s), propulsive impulse (N s), braking peak force (N) and propulsive peak force (N); medio-lateral GRF – positive peak force (N) and negative peak force (N). Also, an absolute error (AE) measure was calculated to visualise the error between measured and estimated GRF as a function of time.

Results

Table 4 details the MD and MV vertical, anterior–posterior and medio-lateral GRF prediction accuracies for subjects A, B, C and D. For both the MLR and ANN models, MV accuracies, as determined by the CC measure, indicate that the vertical (MLR: 0.999, ANN: 0.997) component of GRF can be predicted most accurately, followed by the anterior–posterior (MLR: 0.979, ANN: 0.980), and finally the medio-lateral (MLR: 0.896, ANN: 0.858) component. Further, as verified by both the CC and MAE measures, the MLR model was the most accurate predictor of the vertical (CC: 0.999, MAE: 33.411 N) and medio-lateral (CC: 0.896, MAE: 29.375 N) components of GRF, and the ANN model provided a marginally more accurate prediction of the anterior–posterior (CC: 0.980, MAE: 24.321 N) component of GRF.

Table 5 details the average prediction accuracy, in percent error, for summary parameters commonly employed to describe each component of GRF. In contrast to the above findings the ANN model was able to provide the most accurate MV prediction of vertical GRF (average error: 1.44%) summary parameters. In a similarly contrasting fashion the MLR model provided a marginally superior MV accuracy for anterior–posterior GRF (average error: 6.43%) summary parameter prediction. The contrasting findings detailed in Tables 4 and 5 highlight the fact that the selection of an optimal model was dependent not only on the component of GRF to be predicted, but also on the primary method used for the evaluation of model prediction accuracy (i.e. CC and MAE or summary parameters).

Fig. 6 provides an illustrative example in the case of Subject B for the relationship between measured GRF and ANN and MLR MV predictions for the vertical, anterior–posterior and medio-lateral components of GRF. In this case both the ANN and MLR models are capable of accurately predicting the vertical component of GRF to within an MAE of 18 N. Further, high CC measures (i.e. ANN: 0.999, MLR: 1.000) indicate the close temporal similarity between measured vertical GRF and model predictions.

Utilising the data obtained from Subject B, Fig. 7 illustrates the gait cycle normalised, standard deviation signal (SDs) curve along with the average ANN and MLR absolute error signal (AEs) curve for the vertical, anterior–posterior and medio-lateral components of GRF. The SDs curve was deduced from all nine trials (six MD, three MV) employed for Subject B and hence provided an indication of the overall inherent variability of GRF data. The average AE of model predictions across the three MV trials for Subject B were employed to compute the AEs signal. In general terms, the ANN and MLR AEs curve approximated the SDs curve across the entire gait cycle. This analysis indicated that there is a relationship between the error associated with model predictions (AEs) and the inherent variability of the signal to be predicted (SDs).

Table 3 Optimal artificial neural network (ANN) and multiple linear regression (MLR) model parameters. For both the ANN and MLR models six trials have been used for model development and three trials have been used for model validation.

Model	Model parameter		Optimised parameter
ANN	Training algorithm		Conjugate gradient back-propagation with Fletcher–Reeves updates
	Network structure	Vertical and anterior–posterior GRF	Two hidden layers with 64 neurons in the first hidden layer and 32 neurons in the second hidden layer
		Medio-lateral GRF	Two hidden layers with 128 neurons in the first hidden layer and 64 neurons in the second hidden layer
	Transfer function		Log-sigmoid
	Epoch paradigm		Two MD trial repetitions and 500 MD group repetitions (i.e. 6000 epochs)
	Historical data provision		Current data point along with five preceding data points
MLR	Historical data provision		Current data point along with nine preceding data points

Table 4 Artificial neural network (ANN) and multiple linear regression (MLR) model validation (MV) prediction accuracies, as determined by the correlation coefficient (CC) and mean absolute error (MAE) measures, for vertical, anterior–posterior and medio-lateral components of GRF.

		MLR		ANN	
GRF component	**Subject**	**CC**	**MAE (N)**	**CC**	**MAE (N)**
Vertical (MV)	Subject A	0.999	35.284	0.997	43.821
	Subject B	1.000	16.862	0.999	22.859
	Subject C	0.997	46.658	0.994	55.223
	Subject D	0.999	34.840	0.997	33.475
	Subject av.	**0.999**	**33.411**	**0.997**	**38.845**
Anterior–posterior (MV)	Subject A	0.975	36.141	0.974	31.118
	Subject B	0.991	16.831	0.989	17.809
	Subject C	0.963	35.176	0.973	30.203
	Subject D	0.986	22.763	0.983	18.153
	Subject av.	**0.979**	**27.728**	**0.980**	**24.321**
Medio-lateral (MV)	Subject A	0.911	39.89	0.835	62.168
	Subject B	0.875	29.213	0.912	25.815
	Subject C	0.898	26.914	0.841	39.852
	Subject D	0.901	21.483	0.844	27.764
	Subject av.	**0.896**	**29.375**	**0.858**	**38.900**

Table 5 Artificial neural network (ANN) and multiple linear regression (MLR) model validation (MV) average summary parameter prediction accuracies for vertical, anterior–posterior and medio-lateral components of GRF.

		MLR	ANN
GRF component	**Subject**	**Av. % Error**	**Av. % Error**
Vertical (MV)	Subject A	2.00	1.08
	Subject B	1.50	0.96
	Subject C	2.58	2.13
	Subject D	2.00	1.57
	Subject av.	**2.02**	**1.44**
Anterior–posterior (MV)	Subject A	6.42	5.35
	Subject B	4.16	4.16
	Subject C	10.22	12.27
	Subject D	4.92	4.4
	Subject av.	**6.43**	**6.55**
Medio-lateral (MV)	Subject A	11.65	55.79
	Subject B	38.81	32.22
	Subject C	25.55	30.45
	Subject D	26.19	40.50
	Subject av.	**25.55**	**39.74**

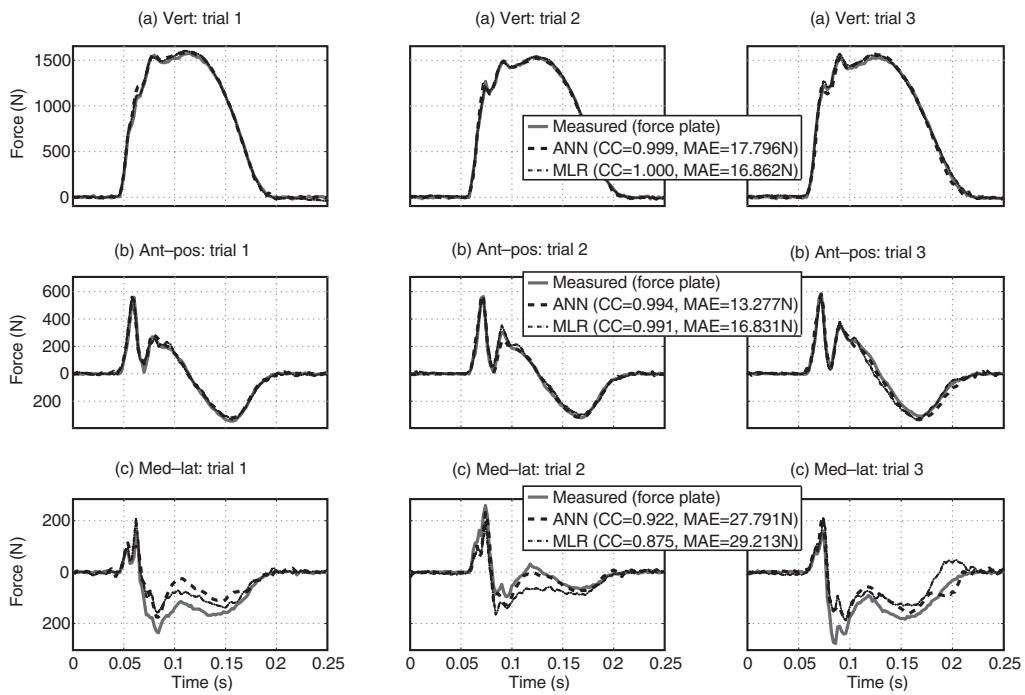

Figure 6 Measured (force plate), artificial neural network (ANN), and multiple linear regression (MLR) model validation (MV) predictions of (a) vertical, (b) anterior–posterior and (c) medio-lateral GRF (subject B).

Discussion

The prediction of the three components of GRF from wearable instrumentation in conjunction with ANN and MLR models in running has not previously been reported in the literature. However, the prediction of the anterior–posterior component of GRF in walking from in-shoe pressure sensors in conjunction with an ANN model has been investigated (Savelberg and de Lange, 1999). A direct comparison to the current study was made difficult due to the use of different data structures and evaluation techniques. However, findings from this study in relation to the accuracy, as determined by the CC measure, in the prediction of the anterior–posterior component of GRF in running (0.973–0.989) may be considered comparable to that reported in the walking domain (0.853–0.963) (Savelberg and de Lange, 1999).

The application of an ANN for modelling gait variable relationships is often justified by the assumption that they can outperform conventional methods of analysis. The concurrent implementation of ANN and MLR models has enabled an assessment for the selection of the preferred model for the prediction of the three components of GRF. In general terms, the MLR model was found to be superior for the prediction of the vertical (CC: 0.999, MAE: 33.411 N) and medio-lateral (CC: 0.896, MAE: 29.375 N) components of GRF and the ANN model was marginally superior for the prediction of anterior–posterior GRF (CC: 0.980, MAE: 24.321 N). However, selection of the preferred model under specific conditions was far more complex and findings that pertain to this research suggest that factors such as the subject-specific inherent signal variability and the method used for the evaluation of model prediction accuracy (i.e. CC and MAE or summary parameters) are important considerations for model selection. When one considers the complexity of implementation and the time consuming process of ANN model optimisation and MD, model selection should also take into consideration the practicality of application. Even if an ANN model was found to provide a nominally higher level of accuracy, the application of a linear model (i.e. MLR) may be justified due to its simplicity and rapidity of implementation.

Studies investigating the prediction of GRF using wearable sensors in conjunction with an ANN have employed the CC measure as the sole time-series means to evaluate GRF prediction accuracy (Savelberg and de Lange, 1999). The CC measure is indicative of the temporal similarity of two signals and

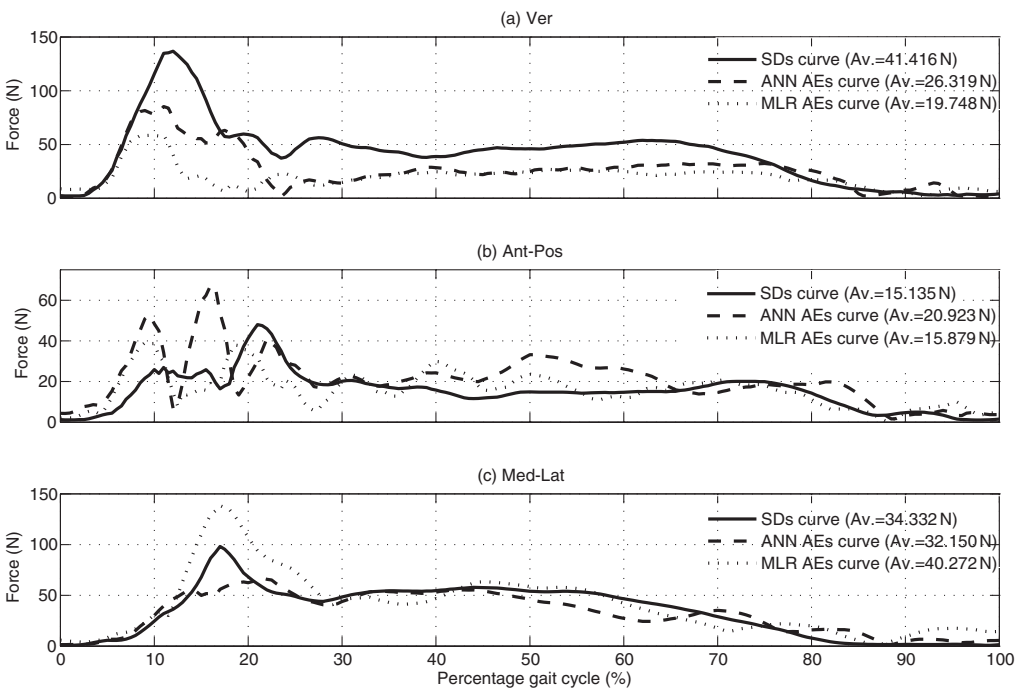

Figure 7 Standard deviation signal (SDs) and absolute error signal (AEs) for artificial neural network (ANN) and multiple linear regression (MLR) model validation (MV) predictions of (a) vertical, (b) anterior–posterior and (c) medio-lateral GRF (Subject B, the average SD across nine trials were employed to compute SDs and average AE across the three MV trials were employed to compute AEs).

is magnitude insensitive. In contrast, the MAE measure indicates the spatial similarity of two signals. In combination the CC and MAE measures provide a complementary indication of the relationship between signals and it is recommended that future studies employ both statistical measures.

It was demonstrated that the inherent variability of target data (SDs) determined throughout the gait cycle was closely approximated by the AEs between MV predictions and measured GRF data. It has therefore been speculated that this inherent signal variability was a governing factor in GRF prediction accuracy. In order to model a system accurately the input parameters should provide information regarding all levels of potential variability of the measure to be predicted. Therefore the GRF prediction accuracies achieved in this research may be improved further through the provision of source data additional to that provided by the existing sensors. For instance, additional hydrocell sensors deployed at other anatomical support structures of the foot (i.e. second and fifth metatarsal head) and or inertial sensors such as accelerometers and gyroscopes to monitor the kinematics of the foot complex may serve to improve GRF prediction accuracies. Furthermore, improvements in the resolution of the wearable instrumentation data through the use of a 10 or 12 bit analogue-to-digital converter may enable a more sensitive relationship between ISF and GRF to be achieved.

Conclusions

The findings of this research provide a proof of concept for the prediction of GRF from wearable instrumentation in middle distance running. The application of this 'hybrid' technique for the collection of continuous GRF records in running has the potential to permit unprecedented insight into athletic performance. In the case of statistical measures of prediction accuracy the MLR model was found to be superior for the prediction of vertical (CC: 0.999, MAE: 33.411 N) and medio-lateral (CC: 0.896, MAE: 29.375 N) components of GRF, whilst the ANN model was found to be best for anterior–posterior GRF (CC: 0.980, MAE: 24.321 N). The prediction accuracy of each component of GRF was found to be governed by the inherent signal variability, in which case the vertical and anterior–posterior components were more reliable and subsequently predicted significantly more accurately than the medio-lateral component.

Owing to the small group of highly skilled, elite study participants involved in this research it is important to acknowledge the constraints within which conclusions from this work can be generalised. Further work is required to investigate the practical application of this technique for the prediction of GRF under training and competition conditions and the suitability for use with other subject populations (i.e. long-distance runners or sprinters). Future work is also required to investigate the predictive capability of ANN and MLR models under conditions where the MV running speeds are above or below MD running speeds (i.e. extrapolation), across different data collection sessions (inter-session), and across different subjects (i.e. inter-subject).

Acknowledgements

The authors would like to express their gratitude to Dr Kynan Graves for his helpful observations and suggestions in the development of the ANN architecture. The authors would also like to thank the Cooperative Research Centre for microTechnology and the Australian Institute of Sport for funding this research.

References

Chau, T. (2001) A review of analytical techniques for gait data. Part 2: neural network and wavelet methods. *Gait & Posture*, **13**, 102–120.

Chesnin, K.J., Selby-Silverstein, L. & Besser, M.P. (2000) Comparison of an in-shoe pressure measurement device to a force plate: concurrent validity of centre of pressure measurements. *Gait & Posture*, **12**, 128–133.

Draper, N.R. & Smith, H. (1998) *Applied regression analysis*. New York, Wiley.

Gross, T.S. & Bunch, R.P. (1989) Discrete normal plantar stress variations with running speed. *Journal of Biomechanics*, **22**, 699–703.

Hennig, E.M. & Milani, T.L. (1995) In-shoe pressure distribution for running in various types of footwear. *Journal of Applied Biomechanics*, **11**, 299–310.

Leyerer, R., Schaff, P. & Wetter, O. (1997) *Device for prevention of ulcers in the feet of diabetes patients*. USA, Paromed Medizintechnik GmbH.

Orlin, M.N. & McPoil, T.G. (2000) Plantar pressure assessment. *Physical Therapy*, **80**, 399–409.

Perttunen, J., Kyrolainen, H., Komi, P.V. & Heinonen, A. (2000) Biomechanical loading in the triple jump. *Journal of Sports Sciences*, **18**, 363–370.

Putnam, C.A. & Kozey, J.W. (1989) Substantive issues in running. In Vaughan, C.L. (Ed.) *Biomechanics of Sport*. Boca Raton, Florida, CRC Press, Inc.

Razian, M.A. & Pepper, M.G. (2003) Design, development, and characteristics of an in-shoe triaxial pressure measurement transducer utilizing a single element of piezoelectric copolymer film. *IEEE Transactions on Neural Systems & Rehabilitation Engineering*, **11**, 288–293.

Savelberg, H.H.C.M. & de Lange, A.L.H. (1999) Assessment of the horizontal, fore-aft component of the ground reaction force from insole pressure patterns by using artificial neural networks. *Clinical Biomechanics*, **14**, 585–592.

Tillman, M., Fiolkowski, P., Bauer, J.A. & Reisinger, K.D. (2002) In-shoe plantar pressure measurements during running on different surfaces: changes in temporal and kinetic parameters. *Sports Engineering*, **5**, 121–128.

Walsh, M. & Kanal, Y. (1997) Measurement of plantar pressure during high impact-short contact time sports activities. *Proceedings of the 15th International Symposium on Biomechanics in Sports*. Denton, Texas.

Weyand, P.G., Sternlight, D.B., Bellizzi, M.J. & Wright, S. (2000) Faster top running speeds are achieved with greater ground forces not more rapid leg movements. *Journal of Applied Physiology*, **89**, 1991–1999.